

See discussions, stats, and author profiles for this publication at: <https://www.researchgate.net/publication/231290914>

Octanol–Air Partition Coefficient for Describing Particle/Gas Partitioning of Aromatic Compounds in Urban Air

ARTICLE *in* ENVIRONMENTAL SCIENCE AND TECHNOLOGY · APRIL 1998

Impact Factor: 5.33 · DOI: 10.1021/es970890r

CITATIONS

311

READS

318

1 AUTHOR:



Tom Harner

Environment Canada

203 PUBLICATIONS 11,369 CITATIONS

SEE PROFILE

Octanol–Air Partition Coefficient for Describing Particle/Gas Partitioning of Aromatic Compounds in Urban Air

TOM HARNER^{*,†}

Department of Chemical Engineering and Applied Chemistry,
University of Toronto, 200 College Street,
Toronto, Ontario M5S 1A4

TERRY F. BIDDLEMAN

Atmospheric Environment Service, 4905 Dufferin Street,
Downsview, Ontario M3H 5T4

Atmospheric concentrations and particle/gas partition coefficients were measured for PAHs, PCBs, and PCNs in urban Chicago during February/March 1995. Average ($n = 15$) concentrations (pg m^{-3}) were $\Sigma\text{PAH} = 58\,000$, $\Sigma\text{PCB} = 350$, and $\Sigma\text{PCN} = 68$. The partitioning of these compounds between the particle phase and the gas phase was investigated and compared to the adsorption (Junge–Pankow) model, which utilizes the subcooled liquid vapor pressure (p_L^0) as a fitting parameter, and the K_{OA} absorption model. The K_{OA} model was able to resolve differences between ortho-chlorine substituted groups of PCBs which correlations against p_L^0 were not able to explain. Partitioning of PCNs was also well described by the K_{OA} model. For PAHs, sorption onto particles agreed with both models when the wind was predominantly from the SW sector. When air was sampled from the NE sector, PAHs showed enrichments in the particle phase relative to the chlorinated aromatics in log–log plots of the particle/gas partition coefficient, K_P versus p_L^0 . Enrichment factors calculated as $K_P(\text{PAH})/K_P(\text{multi-ortho PCB})$ were 27–100 from the NE sector compared to 2–4 for the SW sector. This suggests source region effects on K_P for PAHs. It is hypothesized that the enrichment may be due to nonexchangeable PAHs trapped inside combustion aerosols or a result of a slow re-equilibration of these aerosols as they are diluted in ambient air.

Introduction

Atmospheric transport and particle deposition is an important pathway for the movement of contaminants from urban and industrial centers to nearby lakes (1–4) and distant regions such as the Arctic (5, 6). Semivolatile compounds of concern include PAHs (polycyclic aromatic hydrocarbons), PCBs (polychlorinated biphenyls), and PCNs (polychlorinated naphthalenes) which partition appreciably onto atmospheric particulate matter.

The conventional Junge–Pankow model of particle/gas partitioning assumes that chemicals adsorb to active sites on the surface of the particle. The particle/gas partition coefficient (K_P) is plotted on a log–log scale versus the

subcooled liquid vapor pressure (p_L^0) of the compound (4, 5, 7–9) and the resulting correlations are often quite good. A disadvantage, however, is that different correlations are found among compound classes, and even within a compound class different trends are sometimes observed. For instance, Falconer et al. (10) showed enhanced partitioning (K_P values) for non-ortho (coplanar) PCBs relative to multi-ortho PCBs having the same p_L^0 value.

An alternate absorption model (11, 12) considers that atmospheric aerosols are coated with an organic film. Hence, it is likely that an important aspect of particle/gas partitioning is absorption of chemical into this organic phase. Liang and Pankow (13) found that partitioning of semivolatile compounds to environmental tobacco smoke (almost entirely organic carbon) and urban air particulate matter (~10–20% organic carbon) was nearly the same when normalized to the organic carbon content of the aerosol. Odum et al. (14) modeled the mass transfer of semivolatile organics in and out of combustion aerosols which they described as a solid core coated with a viscous, organic layer.

For several years, K_{OA} has been used to describe plant/air partitioning (15–17), but only recently has it been demonstrated to be a useful descriptor of particle/gas partitioning (18). This paper compares the Junge–Pankow adsorption model with the K_{OA} -based absorption model for describing the particle/gas partitioning of PCBs, PCNs, and PAHs in air samples collected in urban Chicago (February/March 1995).

Experimental Section

Collection of Air Samples. Air samples ($n = 15$) were collected in Chicago approximately 2 km inland from the shore of Lake Michigan on the roof of Farr Hall, Illinois Institute of Technology (IIT), in February/March 1995. A high-volume sampling train consisting of double glass fiber filters (20×25 cm, Gelman A/E) followed by two polyurethane foam (PUF) plugs was used. PUF plugs were precleaned by Soxhlet extraction with acetone (24 h) followed by a second extraction with petroleum ether (24 h) and dried in a vacuum desiccator at ~40 °C (19). Filters were baked at 400 °C for 12 h and then wrapped in aluminum foil and sealed in airtight plastic bags prior to sample collection. PUFs were stored in glass jars with Teflon-lined lids before and after sample collection. Used PUF plugs and glass fiber filters were stored at –10 °C until they were ready to be analyzed.

Chicago samples were taken over 12-h day or night periods to avoid diurnal temperature variations and thereby minimize filtration artifacts. Meteorological data were provided by the Illinois State Water Survey monitoring stations at Farr Hall and Indiana Dunes National Lakeshore near the southern tip of Lake Michigan. Collection information is summarized in Table 1.

A separate sampling train consisting of a single glass fiber filter and two PUF plugs was used for total suspended particle determinations (TSP, μg of particles m^{-3} air). The filters were preweighed after equilibration in a constant humidity chamber for 48 h at 20 °C over a saturated sodium chloride solution. The same procedure was used after sampling to ensure that any changes in filter mass were attributed only to particulate matter and not to differences in water content. The purpose of the PUF plug was to maintain the same flow rate in the TSP sampler as in the train for semivolatile compounds.

Analytical Methods. Air samples were analyzed for PCBs, PCNs, and PAHs. Concentrations of PCNs in air are reported in a previous paper (20). Polyurethane foam plugs were spiked with a mixture of $^{13}\text{C}_{12}$ -labeled mono- and non-ortho

* Corresponding author phone: (416)739-4473; fax: (416)739-5708; e-mail: tom.harner@ec.gc.ca.

† Present address: Atmospheric Environment Service, 4905 Dufferin St., Downsview, ON M3H 5T4.

TABLE 1. Collection Data and Concentrations of Semivolatile Compounds in Chicago

sample	date, 1995	day (D) or night (N)	m ³ air	mean temp (°C)	TSP (μg m ⁻³)	ΣPAH (pg m ⁻³)	ΣPCBs (pg m ⁻³)	ΣPCNs (pg m ⁻³)
1	Feb. 20/21	N	448	3	15	20 000	472	112
2	Feb. 21	D	339	0	34	39 900	359	23
3	Feb. 21/22	N	398	0	60	34 400	294	41
4	Feb. 22	D	337	0	162	102 100	621	87
5	Feb. 22/23	N	445	2	75	48 800	485	92
6	Feb. 23	D	329	4	83	93 000	506	175
7	Feb. 23/24	N	421	0	25	18 100	247	43
8	Feb. 24	D	348	2	34	62 400	208	37
9	Feb. 24/25	N	448	0	41	49 000	316	44
10	Feb. 25	D	325	4	69	41 900	279	24
11	Feb. 25/26	N	425	0	37	25 700	174	28
12	Feb. 26	D	314	0	58	21 400	143	57
13	Feb. 28	D	323	0	123	200 300	588	378
14	Feb. 28/29	N	395	0	87	46 300	282	68
15	Mar. 1	D	320	0	87	65 300	273	87

PCBs 77, 81, 105, 126, and 169 (Cambridge Isotope Laboratories Inc., Andover, MA) and then Soxhlet-extracted overnight with petroleum ether (PE) or hexane. Filters were cut into 1-cm strips and refluxed for the same time period using dichloromethane (DCM). As a quality control step, 200-mg samples of urban air standard reference material 1649 (National Institute of Standards and Technology, Gaithersburg, MD) were placed in precleaned cellulose thimbles and Soxhlet-extracted overnight with DCM.

After volume reduction to 2 mL and transfer to isooctane, the samples were fractionated on a column containing 3 g of silicic acid (3% added water) topped with 2 g of neutral alumina. The column was prewashed with 25 mL of DCM followed by 25 mL of PE. The sample was applied, and PCNs/PCBs were eluted in the first fraction (F1) with 20 mL of PE and the PAHs were eluted in the second fraction (F2) with 20 mL of DCM. Both fractions were reduced by blowing down with a stream of nitrogen.

After an additional cleanup by shaking with 18 M sulfuric acid, F1 was reduced to 1 mL and further fractionated on a minicolumn containing AX-21 activated carbon mixed 1:20 with silicic acid (SA) prepared as described by Falconer et al. (10). The carbon-SA mix (100 mg) was sandwiched between 50-mg layers of SA in a disposable Pasteur pipet containing a small plug of glass wool at the lower end. The column was prewashed with 5 mL of toluene followed by 5 mL of 30% DCM in cyclohexane. The first fraction (F1-1) was eluted with 5 mL of 30% DCM in cyclohexane and contained the multi- and a portion of the mono-ortho PCBs. The second fraction (F1-2) was eluted with 5 mL of toluene and contained PCNs and non-ortho (coplanar) PCBs and the remainder of the mono-ortho PCBs. Both fractions were reduced to 0.2–0.4 mL, and F1-1 was transferred to isooctane.

Analysis. PCNs. PCNs in fraction F1-2 were quantified by GC-negative ion mass spectrometry (GC-NIMS) in selected ion mode (SIM) using NIMS response factors derived from the weight percentages of the individual congeners or congener groups in Halowax 1014, a commercial mixture of PCNs (Reference standard, U.S. Environmental Protection Agency, Research Triangle Park, NC). A more detailed account of the quantification procedure is found elsewhere (20). Ions monitored in SIM mode were (target, qualifier) 3-Cl: 232, 230; 4-Cl: 266, 264; 5-Cl: 300, 298; 6-Cl: 334, 332; 7-Cl: 368, 366; 8-Cl: 404, 402. The criterion for acceptance was a target/qualifier ion ratio within $\pm 20\%$ of the standard. Capillary gas chromatography (GC) was carried out with Hewlett-Packard 5890GC-5989BMS equipped with DB-5MS column (J&W Scientific) with 0.25-mm i.d. and 0.25-μm film thickness, operated with helium carrier gas at 40 cm s⁻¹. Injections (1 μL) were splitless with split opened after 0.5

min and the injector at 250 °C. The temperature program was 90 °C for 0.5 min., 10 °C min⁻¹ to 160 °C, 2 °C min⁻¹ to 250 °C. Other operating conditions were the following: transfer line 250 °C, ion source 150 °C, quadrupole 100 °C, and methane reagent gas at ~ 1.0 Torr.

PCBs. Analysis for PCBs was done in two steps. First, total PCB concentrations were determined from fraction F1 of the silicic acid column. PCB congeners were quantified against a PCB mixture which was prepared from solutions of 56 individual congeners (Accustandard, New Haven, CT). Tribromobiphenyl (Accustandard) was used as the internal standard for volume correction. Quantification was carried out using a Hewlett-Packard 5890 gas chromatograph equipped with an electron capture detector. Peaks were separated on a 60 m DB-5 column (J&W Scientific, 0.25-mm i.d., 0.25-μm film thickness) operated with hydrogen carrier gas at 50 cm s⁻¹. Sample injections (1 μL) were splitless with split opened after 0.5 min and the injector at 250 °C. The temperature program was 90 °C for 0.5 min, 10 °C min⁻¹ to 160 °C, 2 °C min⁻¹ to 250 °C with the detector at 300 °C.

Determination of the mono- and non-ortho PCBs in carbon column fractions F1-1 and F1-2 was performed by GC-NIMS in SIM mode. Ions monitored were (target, qualifier): PCBs 81, 77 (292, 290); PCBs 118, 114, 105, 126 (326, 324); PCBs 156, 169 (360, 358); [¹³C₁₂]PCBs 81, 77 (304, 302); [¹³C₁₂]PCB 126 (338, 336); [¹³C₁₂]PCB 105 (340, 338); [¹³C₁₂]PCB 169 (372, 370). Ions 289 and 291 were monitored for PCB 103 which was used as the internal standard for volume correction. GC and MS conditions and temperature program were the same as for the analysis of PCNs.

PAHs. Samples ($n = 15$) were analyzed by GC-electron impact MS with the source at 200 °C and quadrupole at 100 °C. GC conditions were the same as for PCNs. Quantification was performed using a calibration solution of 16 PAH compounds (EPA method 610/8310, AXACT, Commack, NY 11725). Deuterated chrysene (Cambridge Isotope Laboratories, Andover, MA) was added as internal standard for volume correction. Ions monitored were (target, qualifier) as follows: fluorene (166, 165), phenanthrene, anthracene (178, 176), fluoranthene, pyrene (202, 200), chrysene-*d*₁₂ (240, 241), benz[*a*]anthracene, chrysene (228, 226), benzo[*b*]fluoranthene, benzo[*k*]fluoranthene, benzo[*a*]pyrene (252, 250), indeno[1,2,3-*cd*]pyrene, dibenz[*ah*]anthracene, benzo[*ghi*]perylene (276, 138). The 3–4 ring compounds were determined on both PUFs and filters, while 5–6 ring compounds were determined on filters only.

Results and Discussion

Quality Control. At the sampling site, several PUF plugs and filters were spiked with PCNs (Halowax 1014) and a

standard solution of 56 PCB congeners. All samples, including spikes, were fortified prior to extraction with a surrogate standard solution containing several isotopically labeled ($^{13}\text{C}_{12}$) mono-ortho and non-ortho PCBs. The surrogate was applied to PUFs which were contained in the Soxhlet apparatus just prior to extraction. In the case of the filters the surrogate was applied in small drops to the surface of the filter which was then cut into 1-cm wide strips and refluxed with DCM. Recoveries of PCBs and PCNs from PUF plugs were 80–120% and 50–80%, respectively. Recoveries from filters were of similar magnitude for the higher molecular weight congeners but substantially reduced for the lower molecular weight PCBs (2-Cl and 3-Cl) and PCNs (3-Cl and 4-Cl). Subsequent laboratory tests attributed these low recoveries to evaporation when the surrogate was applied to the surface of the filter. Hence, PUF surrogate recoveries were used for both PUF and filter samples.

F1 from the silicic acid column was reduced to 1 mL and analyzed by GC-ECD for all PCBs. Spike recoveries for this fraction ranged from 80 to 120%. Carbon column fractions F1-1 and F1-2 were reduced to approximately 0.2 mL to increase the detectability. Evaporative losses for the mono- and non-ortho PCBs were accounted for by the recovery factors for $^{13}\text{C}_{12}$ -labeled PCB 81, 77, 126, 169, and 105, which were specific to each sample. Recoveries of these ranged from 50 to 85%. Recoveries for PCNs ranged from 50% for the 3-Cl congeners to 80% for the heavier congeners. Method recoveries for PAHs were determined by spiking clean PUF plugs in the laboratory with the PAH standard solution and then treating the PUF as a sample. PAHs were contained in fraction F2 of the silicic acid separation and mean ($n = 3$) recoveries were the following: fluorene $72 \pm 11\%$, phenanthrene $93 \pm 8\%$, anthracene $93 \pm 6\%$, fluoranthene $100 \pm 8\%$, pyrene $95 \pm 7\%$, benz[a]anthracene $87 \pm 6\%$, chrysene $99 \pm 8\%$, benzo[b]fluoranthene $75 \pm 7\%$, benzo[k]fluoranthene $83 \pm 9\%$, benzo[a]pyrene $72 \pm 5\%$, indeno[1,2,3-*cd*]pyrene $73 \pm 5\%$, dibenz[ah]anthracene $67 \pm 7\%$, and benzo[ghi]perylene $82 \pm 8\%$.

Average ($n = 6$) recoveries of 10 PCBs and 11 PAHs from NIST urban dust were 84–125% for PCBs [using NIST values from Shantz et al. (21)] and 42–127% for PAHs [using NIST values from Wise et al. (22)]. Individual recoveries are listed: PCB 28, $84 \pm 18\%$; PCB 31, $114 \pm 20\%$; PCB 52, $86 \pm 8\%$; PCB 101, $125 \pm 8\%$; PCB 105, $126 \pm 11\%$; PCB 118, $86 \pm 7\%$ (GC-MS, $110 \pm 9\%$); PCB 138/137, $84 \pm 4\%$; PCB-153 $98 \pm 5\%$; PCB-156 $91 \pm 11\%$; PCB-180 $99 \pm 2\%$; phenanthrene $49 \pm 3\%$; anthracene, $64 \pm 17\%$; fluoranthene, $42 \pm 3\%$; pyrene, $47 \pm 3\%$; benz[a]anthracene, $57 \pm 3\%$; chrysene, $58 \pm 5\%$; benzo[b]fluoranthene, $122 \pm 13\%$; benzo[k]fluoranthene, $128 \pm 21\%$; benzo[a]pyrene, $97 \pm 18\%$; indeno[1,2,3-*cd*]pyrene, $101 \pm 22\%$; benzo[ghi]perylene, $85 \pm 14\%$.

Quantities of semivolatile compounds on back PUF plugs were used to correct the samples for blanks. These were expressed as concentrations by dividing by the sample air volume. Field blanks were also collected at the sample location by periodically placing a clean PUF plug in the sample train and then restoring it to the glass sample jar. The larger of these two blank values was used for sample correction. Limit of detection values ($\text{LOD} = \text{blank} + 3 \text{ SD}$) for individual compounds were in the following ranges: PAHs $0.01\text{--}0.1 \text{ ng m}^{-3}$, PCBs $0.03\text{--}3 \text{ pg m}^{-3}$, and PCNs approximately 0.025 pg m^{-3} . Since PCNs were virtually nondetectable in the blanks, LOD values were calculated on the basis of the area of the smallest peak that could be integrated. Samples exceeding LOD values were corrected for average blanks and method recovery factors.

Ambient Air Concentrations of PAHs, PCBs, and PCNs.

Atmospheric concentrations of PAHs, PCBs, and PCNs in Chicago are listed in Table 1, with corresponding average mass percent distributions summarized in Figure 1.

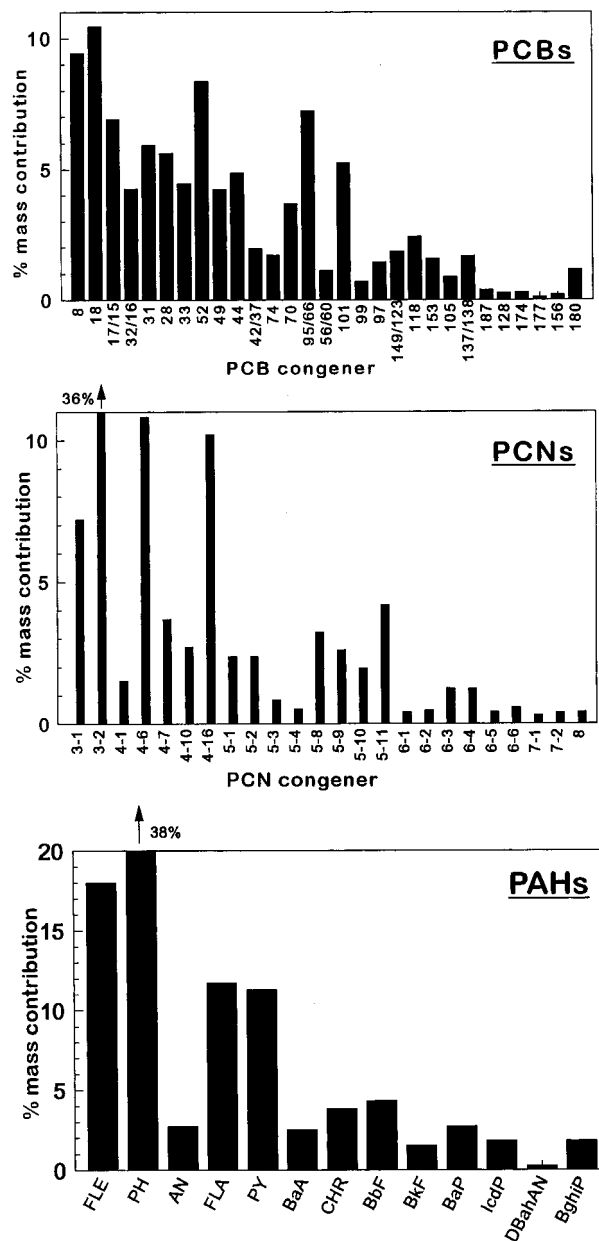


FIGURE 1. Mass percent contributions of PAHs, PCBs, and PCNs in Chicago air. (PAHs: FLE, fluorene; PH, phenanthrene; AN, anthracene; FLA, fluoranthene; PY, pyrene; BaA, benz[a]anthracene; CHR, chrysene; BbF, benzo[b]fluoranthene; BkF, benzo[k]fluoranthene; BaP, benzo[a]pyrene; IcdP, indeno[1,2,3-*cd*]pyrene; DBahAN, dibenz[ah]anthracene; BghiP, benzo[ghi]perylene).

PAHs had the highest levels of the three compound classes, with mean $\Sigma\text{PAH} = 58 \text{ ng m}^{-3}$. The mass distribution was dominated by fluorene, phenanthrene, fluoranthene, and pyrene, while other PAHs individually accounted for less than 2% of the total (Figure 1). These data are approximately a factor of 3 lower than measurements taken in a heavily industrialized region of Chicago in February 1988 (9) and are in the same range as reported by Simcik et al. (23) for air samples collected at the IIT site 3 weeks prior to this study ($\Sigma\text{PAH} = 51\text{--}162 \text{ ng m}^{-3}$).

The average value for ΣPCB in Chicago was 350 pg m^{-3} . Again, PCB levels were about 5 times lower than previous measurements taken near a more heavily industrialized region in Chicago (9) and within the same range (i.e., $270\text{--}910 \text{ pg m}^{-3}$) as values reported by Simcik et al. (23). The mass profile of PCBs in Chicago was dominated by the tri- and tetrachlorinated biphenyls (Figure 1).

TABLE 2. Mean Particulate Percentages of PCBs, PCNs, and PAHs in Chicago Air Samples

PCB	% particulate	PCN	% particulate	PAH ^a	% particulate
3-Cl	7.3	3-Cl	1.3	3-ring	4.4
4-Cl	16.7	4-Cl	6.2	4-ring	42.9
5-Cl	34.7	5-Cl	28.6		
6-Cl	58.3	6-Cl	70.2		
7-Cl	66.2	7-Cl	77.0		
8-Cl	79.5	8-Cl	98.5		

^a Particulate percentages of 5–6 ring compounds were not determined, since only the filters were analyzed for these compounds.

Results for PCNs represent the first reported air concentrations for this class of compounds near the Great Lakes (20). The average value for Σ PCN was 68 pg m^{-3} , excluding one high value (378 pg m^{-3}) which was taken when the wind was coming from a local source. The air profile was dominated by the 3-, 4-, and 5-chlorinated (Cl) congeners as shown in Figure 1, where the first number represents the homologue group (3-Cl, 4-Cl, etc.) and the second is its elution order within that group on a DB-5 column. Identities of individual congeners are given by Harner and Bidleman (20, 24). One of the 3-Cl congeners (2,4,6-trichloronaphthalene) accounted for more than 35% of the total mass. This may reflect the large market share (65%) of the technical mixtures Halowax 1001 and 1099 which consist of 80% 3- and 4-Cl congeners.

Several PCNs exhibit dioxin-like toxicity, and tetrachloro-*p*-dibenzodioxin toxic equivalent factors (TEFs) have been reported for several 6-Cl and 7-Cl congeners which were quantified in this study (25). These include PCN 66+67 (1,2,3,4,6,7/1,2,3,5,6,7 TEF = 0.002), PCN 69 (1,2,3,5,7,8 TEF = 0.002), PCN 63 (1,2,3,4,5,6 TEF = 0.002), and PCN 73 (1,2,3,4,5,6,7 TEF = 0.003). Mean values for these congeners in Chicago air (pg m^{-3}) were 0.32 ± 0.36 (PCN 66+67), 0.81 ± 1.57 (PCN 69), 0.21 ± 0.15 (PCN 63), and 0.25 ± 0.28 (PCN 73). Hanberg et al. (25) also report TEFs for coplanar PCBs and PCB 105, which are believed to be among the most dioxin-like of the PCB congeners. TEFs are 0.0005 (PCB 77), 0.1 (PCB 126), and 0.0001 (PCB 105). Levels of these compounds in the Chicago samples were (pg m^{-3}) 0.42 (PCB 77), 0.063 (PCB 126), and 3.27 (PCB 105). Relative dioxin-like toxicity contributions of different compounds can be compared by calculating TCDD toxic equivalents (TEQ = TEF \times air concentration). For the average Chicago sample, the relative TEQ contributions are 61.5% (PCB 126), 2% (PCB 77), 3.2% (PCB 105), and 33.3% (PCNs combined). Most of the dioxin-like toxicity is attributed to PCB 126. There is also a large TEQ contribution for PCNs, and further investigation of this compound class is merited.

Particle–Gas Partitioning of PAHs, PCBs, and PCNs in Chicago Air. Semivolatile aromatics such as PAHs, PCBs, and PCNs are present in the gas phase and attached to particles. Table 2 shows average particulate percentages of the various homologue groups for PCBs, PCNs, and PAHs. It is a common practice to describe the phase distribution using the particle/gas partition coefficient, $K_p = C_p / C_g$ (4, 9, 26, 27). The fraction (ϕ) of compound in the particle phase is

$$\phi = C_p(\text{TSP}) / [C_g + C_p(\text{TSP})] = K_p(\text{TSP}) / [1 + K_p(\text{TSP})] \quad (2)$$

where C_p is the concentration on particles ($\text{ng } \mu\text{g}^{-1}$ of particles), C_g is the gas-phase concentration (ng m^{-3} of air), and TSP is the total suspended particle concentration (μg

m^{-3}). To partially correct for adsorption of gaseous compound to the filter, C_p and C_g were calculated from

$$C_p = (\text{FF} - \text{BF}) / \mu\text{g of particles} \quad (3)$$

where FF and BF are the quantities of chemical on the front

$$C_g = (\text{PUF} + 2\text{BF}) / \text{m}^3 \text{ of air} \quad (4)$$

and back glass fiber filters, and PUF is the quantity found on the polyurethane foam plug (9, 28, 27).

The particle/gas partition coefficient is often correlated with the subcooled liquid vapor pressure (p_L^0) using eq 5.

$$\log K_p = m \log p_L^0 + b \quad (5)$$

Under equilibrium conditions and for compounds of the same class, the expected slope (m) of eq 5 is -1 . Interpretation of the intercept term (b) depends on the assumed mechanism of particle–gas interaction. If compounds are adsorbed to active sites on the particle surface, b is related to the specific surface area of the particle and the excess heat of desorption from the particle surface (7, 26). If the mechanism is absorption into a liquidlike film on the aerosol, b depends on the fraction of organic matter in the particle that is involved in the partitioning process and the activity coefficient of the compound in the organic film (11). Sampling artifacts and/or nonequilibrium conditions may lead to values of $m \neq -1$ (8, 9).

Figure 2 (A series) shows log–log plots of K_p versus p_L^0 for PAHs (fluorene, phenanthrene, fluoranthene, pyrene) and PCBs in Chicago air. PCNs are not included since no congener-specific vapor pressure data are available. The plots show enhanced sorption to the particle phase for PAHs relative to the multi-ortho PCBs. The correlations are made using liquid-phase vapor pressures from Falconer et al. (20) for PCBs and Yamasaki et al. (30) for PAHs. Both sets of vapor pressures are based on GC retention data. The enhancement of PAHs over PCBs is slightly greater if the PAH vapor pressures of Hinckley et al. (31) are used. The latter are based on GC-retention data or conversion of solid- to liquid-phase vapor pressures, and are ~ 2 – 3 times higher than Yamasaki's values.

The reason for this enhancement is not clear. A possibility for PAHs is that during their formation in combustion some PAHs become bound within the particle and are nonexchangeable with the atmosphere. Some of this PAH pool may be extracted during analysis, however. The nonexchangeable effect usually causes curvature in plots of eq 5 (28, 32), although the number of PAH points in Figure 2 (A series) is insufficient to see this effect if it were present. PCBs, on the other hand, are likely to partition onto particles already present in air and may more easily approach a true equilibrium. In other words, the discrepancy between PAHs and PCBs may be explained by their being bound in different ways or even to different types of particles, with the PAHs skewed toward particles originating from combustion sources. The heat of desorption from the particle surface may also be greater for PAHs than for PCBs (7).

Enrichment factors (EFs) for PAHs were determined from log–log plots of K_p versus p_L^0 . EF values were calculated by considering the deviation of a PAH point from the least-squares line that was fitted through the multi-ortho PCBs, i.e., $K_p(\text{PAH}) / K_p(\text{multi-ortho PCB})$. Figure 3a shows that the largest EFs were found for samples which contained more than 50% contribution of air from the NE sector (315° – 135°) ($n = 9$). This sector represents downtown Chicago. Geometric mean EF values for air containing greater than 50% NE sector air were fluorene (60), phenanthrene (30.2), fluoranthene (18.1),

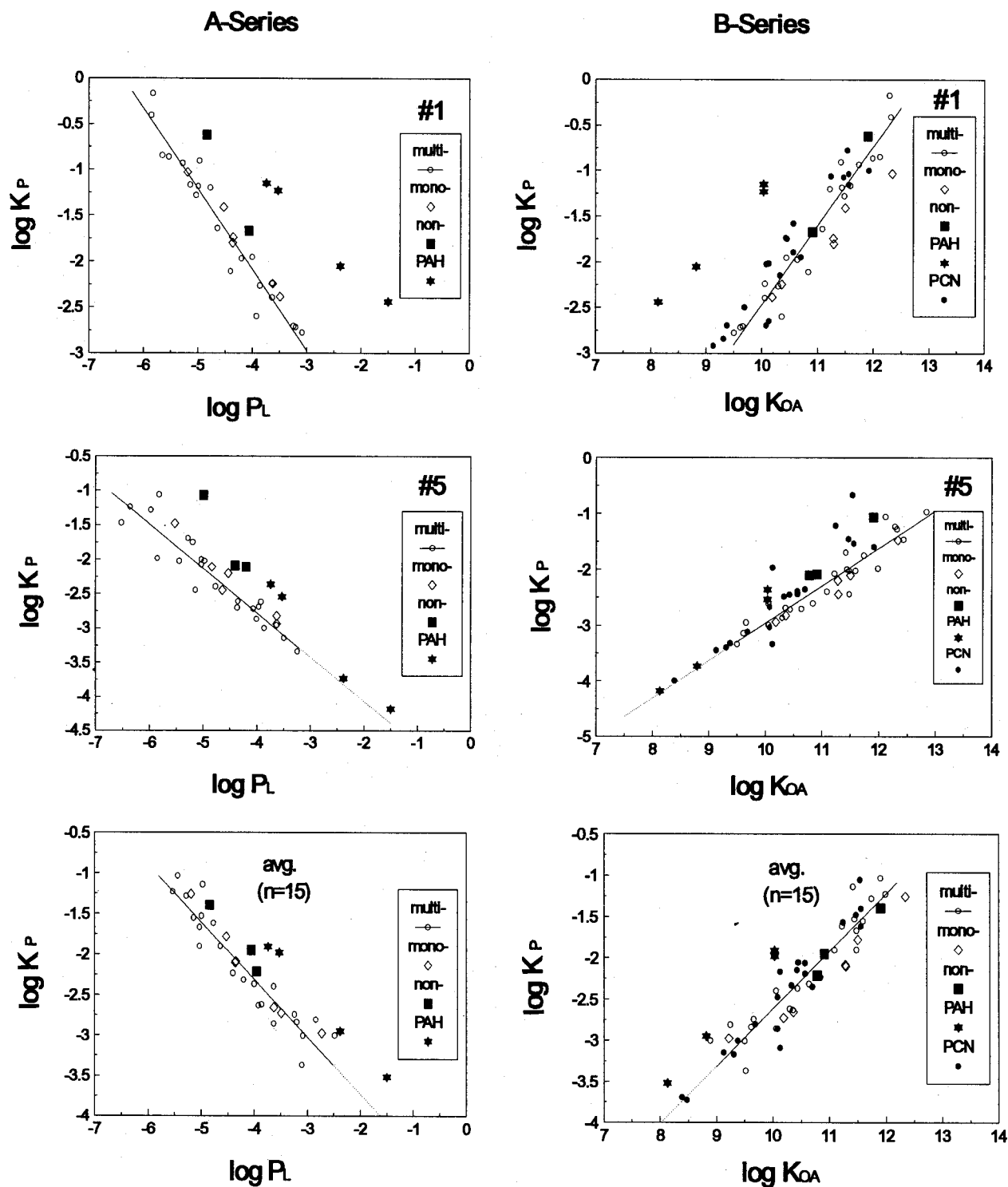


FIGURE 2. Log-log plots of K_p against p_L° (Pa) (A series) and K_{OA} (B series) for PAHs (FLE, PH, FLA, and PY), multi-ortho PCBs, mono-ortho PCBs, non-ortho PCBs, and PCNs (K_{OA} only). Air samples #1 and #5 were selected because they show large and moderate enrichment of PAHs over PCBs. Note that differences in partitioning between the multi- and non-ortho PCBs are minimized in the B series plots. Regression lines are for multi-ortho PCBs.

and pyrene (16.5). For 100% NE sector air ($n = 4$) the EF values were fluorene (100), phenanthrene (47.4), fluoranthene (27.8), and pyrene (27.1).

In contrast, much smaller particle-phase enrichments were observed for PAHs in air originating from the SW sector (135° – 315°). This sector represents a mix of residential and heavily industrial regions. Geometric mean EF values for samples containing > 50% SW sector air ($n = 6$) were fluorene (2.4), phenanthrene (2.2), fluoranthene (3.8), and pyrene (3.0).

For 100% SW sector air ($n = 3$), the EF values were fluorene (2.1), phenanthrene (2.5), fluoranthene (4.0), and pyrene (3.4). Cotham and Bidleman (9) found that PAHs were sorbed to a greater extent than PCBs in the south Chicago industrial section. From their log-log correlations of average K_p vs p_L° , the EFs for PAHs are 2.6–3.5, similar to what is observed in this study during transport from the SW sector.

These results suggest that the K_p values for PAHs are dependent on source region and hence aerosol type.

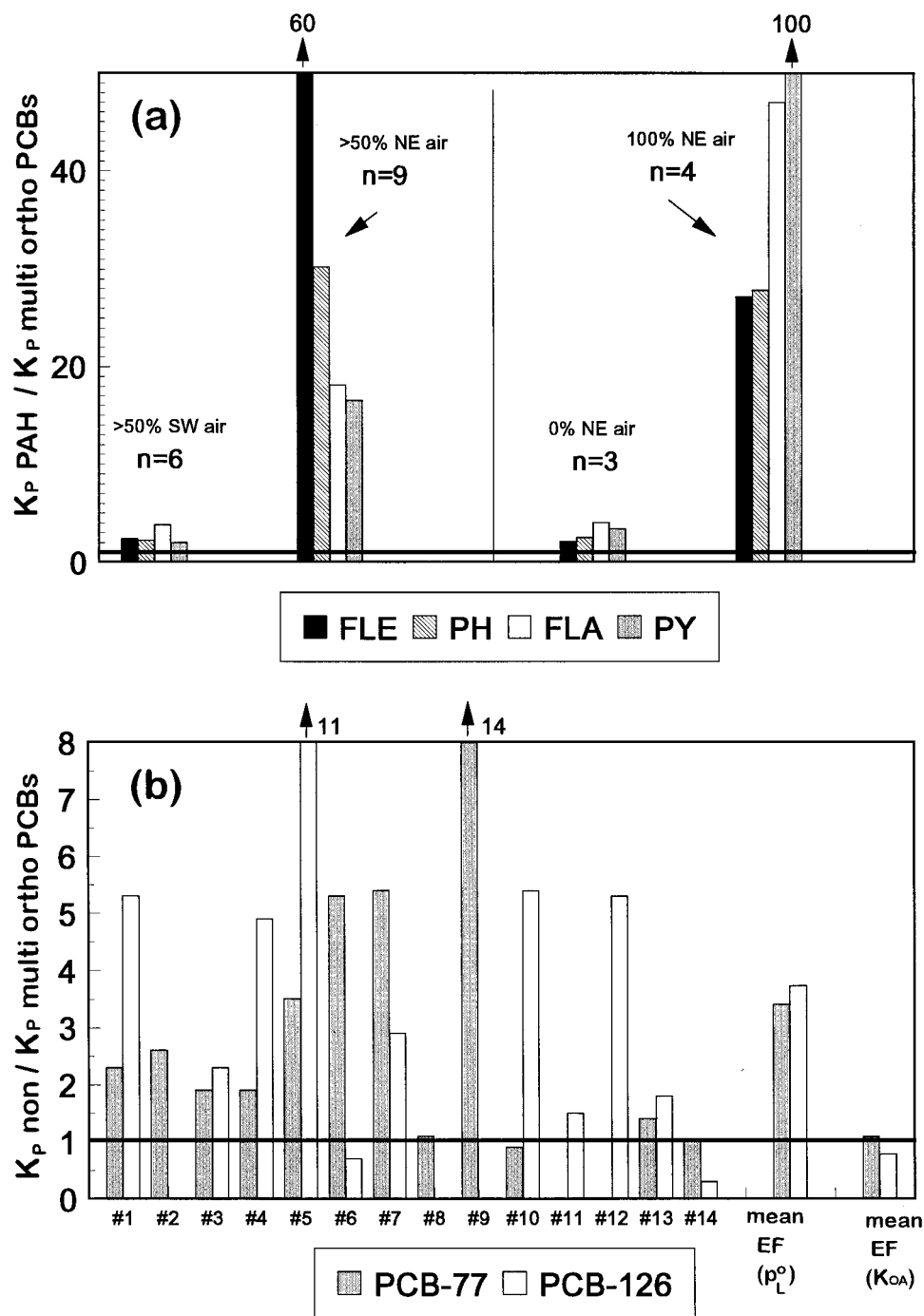


FIGURE 3. Particle/gas partition coefficient enrichment factors in Chicago air samples. (a) PAHs, where $EF = K_{P(\text{PAH})} / K_{P(\text{multi-ortho PCB})}$. Note the differences in EF values for PAHs depending on aerosol source region—NE sector (315° to 135°) air versus SW sector (135° to 315°) air. (b) PCBs, where $EF = K_{P(\text{non-ortho PCB})} / K_{P(\text{multi-ortho})}$ determined from plots of $\log K_P$ versus $\log p_L^\circ$ and $\log K_P$ versus $\log K_{OA}$. No significant enrichment is seen for the latter.

Inspection of data from a study by Holsen et al. (33) at the same sampling location revealed a connection between aerosol type and wind direction. They found that when the air came from the SW sector 15% of the time, coarse particles ($2.5\text{--}10\text{ }\mu\text{m}$) accounted for 40% of the total particle mass. This increased to 57% when the air arrived from the SW 30% of the time. The samples with greater contributions of SW sector air also had higher levels of calcium which is indicative of crustal origin. Hence, at this sampling location, the SW sector appeared to contribute more larger particles which were primarily a result of mechanical abrasion and erosion. Conversely, samples for which the contribution of NE sector air was greater had higher proportions of fine particles (<2.5

μm) due to combustion ($<0.1\text{ }\mu\text{m}$) and accumulation mode ($0.1\text{--}2.5\text{ }\mu\text{m}$) aerosols (33).

In summary, higher K_P values for PAHs (relative to multi-ortho PCBs) were found for Chicago aerosols. The EFs were on the order of 2–4 for air arriving from the SW sector and significantly higher (27–100) when the wind was from the NE. We speculate that aerosol size distribution may be related to these differences, but no conclusions can be drawn without information on the particle size distributions of PAHs and PCBs. Other complicating factors may be the presence of some nonexchangeable PAHs in the particles (32) and slow re-equilibration of combustion aerosols as they are diluted in ambient air. Kamens et al. (34) showed that under cool,

outdoor conditions (-1 to -4°C), tens of hours were required for compounds such as phenanthrene and pyrene to reestablish 90% of equilibrium once they had departed from equilibrium in the particle phase.

Figure 2 (A series) plots also show enhanced partitioning for coplanar PCBs relative to the least-squares line for the multi-ortho congeners. Preferential sorption of coplanar PCBs was also found in a previous study of aerosols from southeast Chicago (10). In this case, the authors were able to account for the enrichment by the more nearly planar configuration of the non-ortho and mono-ortho PCBs.

It may be a physical characteristic of non-ortho PCBs which gives them a partitioning advantage compared to other PCBs. As seen in Figure 2 (A series), vapor pressure is not able to explain this effect. Rather than adsorbing to active sites on the particle surface, it is possible that the chemical is actually absorbing or dissolving into an organic layer on the particle (11). Aerosols contain about 10% organic carbon and greater amounts of organic matter. The organic matter on aerosols is a mixture of nonpolar compounds and polar material that is formed by oxidation and gas-to-particle conversion, i.e., "secondary organic aerosol" (12, 34, 35). If absorption is the dominant process, a more appropriate descriptor may be the octanol-air partition coefficient, K_{OA} (18, 43).

Figure 2 (B series) shows log-log plots of K_P versus K_{OA} . In these plots, the non-ortho PCBs which fell above the multi-ortho line in the p_L° correlation (A series) now fall in line with the rest of the PCBs. The ability of K_{OA} to resolve the difference in the PCB types is further illustrated in Figure 3b. Enrichment factors ($EF = K_{P(\text{non-ortho})}/K_{P(\text{multi-ortho})}$) for the non-ortho PCBs (congeners 77 and 126) were calculated for all air samples. $K_{P(\text{multi-ortho})}$ values were taken from regression lines of individual sample events, e.g., in Figure 2 (A series) plots. Several (although not all) of the samples showed enrichment of the coplanar PCBs. The mean EFs for PCB 77 and 126 were approximately 3.4 and 3.7 and indicate that these congeners partition onto particles 3.4 to 3.7 times more strongly than a multi-ortho PCB having the same vapor pressure (see Figure 3b). A t -test showed that these mean EFs were significantly different than unity with p -values < 0.05 for both congeners. Enrichment factors were also calculated for plots of log K_P versus log K_{OA} . The mean EFs (the last bar in Figure 3b) for PCB 77 and 126 are close to unity, indicating that the enrichment of the non-ortho PCBs has been resolved by K_{OA} . The same t -test for these plots resulted in p -values of $p > 0.8$ and $p > 0.35$, indicating that the K_{OA} -based EFs are not significantly different from unity.

Partitioning onto particles for another class of chlorinated aromatics—PCNs—was also well described by K_{OA} (Figure 2, B Series). These results encourage the use of K_{OA} as a particle/gas partitioning descriptor and support the hypothesis that the mechanism of particle/gas partitioning for the chlorinated aromatics is absorption into an organic film which coats atmospheric particulate matter.

As discussed earlier, PAHs, which have planar structures, also have higher K_P values than nonplanar PCBs of the same vapor pressure (Figure 2, A Series; and Figure 3a). This enrichment cannot be resolved by K_{OA} (Figure 2, B Series) since PAHs do not appear to show preferential absorption into octanol compared to multi-ortho PCBs (24). This suggests some other explanation, as discussed earlier.

The regression equations for log-log correlations of average K_P ($n = 15$) against K_{OA} and p_L° are as follows:

(all PCBs):

$$\log K_P = 0.654 \log K_{OA} - 9.183; r^2 = 0.876; n = 33$$

(PCNs):

$$\log K_P = 0.735 \log K_{OA} - 9.947; r^2 = 0.918; n = 22$$

(PAHs):

$$\log K_P = 0.829 \log K_{OA} - 10.263; r^2 = 0.999; n = 4$$

and

(all PCBs):

$$\log K_P = -0.715 \log p_L^\circ - 5.141; r^2 = 0.886; n = 33$$

(PAHs):

$$\log K_P = -0.745 \log p_L^\circ - 4.666; r^2 = 0.999; n = 4$$

Models of Particle/Gas Partitioning—Adsorption versus Absorption. Junge–Pankow Adsorption Model. First proposed by Junge (38) and later critically reviewed by Pankow (7), the Junge–Pankow model (eq 6) is the most common method for estimating adsorption of semivolatile organic compounds to aerosols.

$$\phi = c\theta/(p_L^\circ + c\theta) \quad (6)$$

This model relates the fraction of chemical adsorbed to particles (ϕ) to the subcooled liquid vapor pressure of the pure compound (p_L° , Pa) and the particle surface area per unit volume of air (θ , cm^2 of aerosol cm^{-3} of air). The parameter c (Pa cm) is based on the heat of desorption from the particle surface, the heat of vaporization of the compound, and the moles of adsorption sites on the aerosol. A value of $c = 17.2$ Pa cm is typically used, although Pankow (7) suggests that this may vary with the class of compound. Values for the surface area parameter, θ , are often assumed to be 1.1×10^{-5} for urban air and $(4.2-35) \times 10^{-7}$ for rural air (39).

Absorption Model. It has been recently proposed by Pankow (11, 12) that absorption of gas-phase compounds into an organic film coating the particle makes an important contribution to the overall particle–gas partitioning process. Pankow's expression for K_P based on absorption is

$$K_P = 10^{-6} RT f_{om} / M_{om} \gamma_{om} p_L^\circ \quad (7)$$

where f_{om} is the fraction of the particle mass that consists of absorbing organic matter having molecular weight M_{om} (g mol^{-1}) and activity coefficient γ_{om} in the organic film ($\gamma_{om} \rightarrow 1$ as $X \rightarrow 1$, Raoult's Law). A substantial portion of this organic matter may be secondary organic aerosol, which is formed by oxidation of hydrocarbons and is therefore polar (12). A problem with the absorption model is that γ_{om} is not often known, and recent work (13, 49) suggests that this quantity may vary substantially among different classes of compounds.

K_{OA} Absorption Model. A logarithmic form of eq 7 is

$$\log K_P = \log f_{om} + \log 10^{-6} RT / M_{om} \gamma_{om} p_L^\circ \quad (8)$$

where the term $10^{-6} RT / M_{om} \gamma_{om} p_L^\circ$ is related to the partition coefficient of the compound between the organic matter and air. This suggests using the octanol–air partition coefficient (K_{OA}) as an alternative to vapor pressure for describing absorption to aerosols (18, 37, 40, 43). Values of K_{OA} have been reported as a function of temperature for several PCB congeners, chlorobenzenes, PAHs, and polychlorinated naphthalenes (PCNs) (24, 37, 40, 41).

The relationship of K_P to K_{OA} is (18, 43)

$$K_P = 10^{-9} K_{OA} f_{om} (\gamma_{oct} / \gamma_{om}) (M_{oct} / M_{om}) / \rho_{oct} \quad (9)$$

where f_{om} is the fraction of organic matter in the aerosol

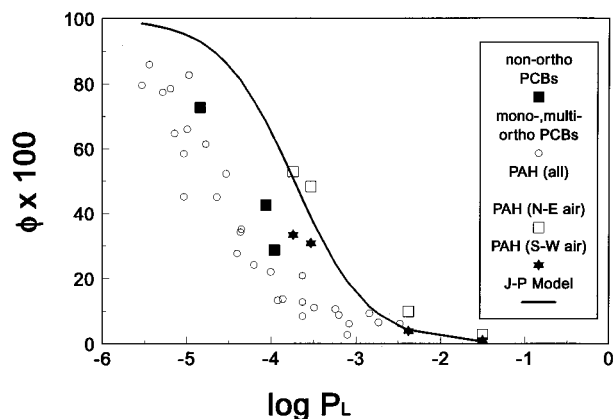


FIGURE 4. Junge–Pankow adsorption model of particulate percentage ($\phi \times 100$) (solid line) compared to observed particulate percentages for PAHs and PCBs as a function of vapor pressure, p_L° (Pa).

involved in partitioning, γ_{oct} and γ_{om} are the activity coefficients of the absorbing compound in octanol and aerosol organic matter, M_{oct} and M_{om} are the molecular weights of octanol (130 g mol^{-1}) and the organic matter, and ρ_{oct} is the density of octanol (820 kg m^{-3}). With the assumptions that γ_{oct}/γ_{om} and $M_{oct}/M_{om} = 1$:

$$\log K_p = \log K_{OA} + \log f_{om} - 11.91 \quad (10)$$

The K_{OA} absorption model (eq 10) can be used to predict values of K_p from knowledge of only K_{OA} and the organic fraction of the aerosol, f_{om} , if it is further assumed that all of the aerosol organic matter is available to absorb gaseous compounds. The fraction on particles (ϕ) is then calculated from K_p and TSP by eq 2.

Comparison of Adsorption and K_{OA} Absorption Models.

Figure 4 compares the percent ($\phi \times 100$) on particles as predicted by the Junge–Pankow adsorption model (using $c = 17.2 \text{ Pa cm}$ and $\theta = 1.1 \times 10^{-5}$) with the average experimental values for PCBs and PAHs ($n = 15$). PCNs are not included due to the lack of p_L° values. The Junge–Pankow model gives particulate percentages for PAHs which are in good agreement with sampling data, but overpredicts sorption of PCBs. The same trend was found in an earlier study in south Chicago (9). Comparisons of several data sets from urban and rural locations also show that sorption of PAHs is well represented by the Junge–Pankow approach (36, 42, 43).

Agreement between the model and sampling results is no guarantee that either gives the correct result. Filtration air samplers are subject to “blow off” artifacts which result in loss of semivolatile compounds from filtered particles. Parallel experiments with denuders yield higher particulate fractions for PAHs (44, 45). In the Junge–Pankow model, θ can be expected to vary with aerosol size distribution (46) and Q_d may vary for different compound classes (7, 47).

The K_{OA} absorption model can be applied in the same manner using eq 10 and the organic matter content of the aerosols. Shah et al. (48) reported an average organic carbon content of airborne particles in U.S. cities of 8.4%. Cotham and Bidleman (9) reported total carbon (organic + elemental) levels of 23% in Chicago urban aerosol. This corresponds to 15% organic carbon if an organic/elemental ratio of 1.8 is assumed (48). Conversion from organic carbon to organic matter is possible if we assume that organic compounds present on urban aerosols have, on average, the molecular formula of octanol (74% carbon). Hence, 15% organic carbon corresponds to approximately 20% organic matter.

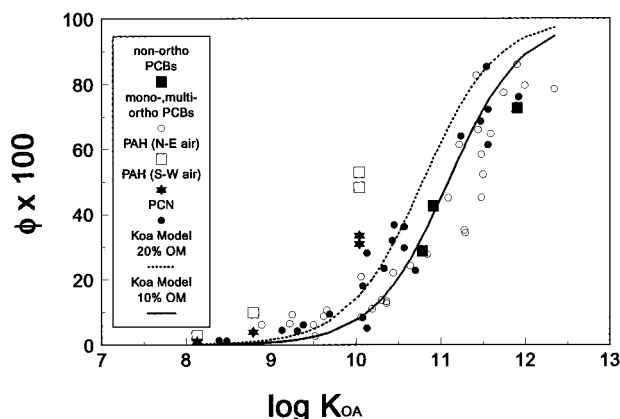


FIGURE 5. Absorption model of particulate percentages (solid and dashed lines) compared to observed particulate percentages for PAHs and PCBs as a function of K_{OA} for an aerosol containing 10% and 20% organic matter.

Figure 5 shows the particulate fractions predicted by the absorption model assuming organic matter fractions of 10% and 20%, which are in the range expected for urban aerosols. The K_{OA} model fits the PCB data better than the Junge–Pankow model, resolves differences between multi-ortho and non-ortho PCBs, and also explains the partitioning data for PCNs. The particle/gas distribution of PAH is underpredicted (see also Figure 2, B-series; and 3b). As hypothesized earlier, this may be related to the presence of nonexchangeable PAHs or due to the long times required for aerosol–air reequilibration.

It is increasingly accepted that partitioning of semivolatile organics to “environmental lipids” (soil, vegetation, aerosols) is controlled by an absorptive rather than, or in addition to, an adsorptive mechanism. The octanol–air partition coefficient is a good descriptor for the partitioning of PCBs and PCNs between the air and atmospheric particulate matter. Correlations of K_p against K_{OA} are able to resolve differences between the ortho-chlorine substitution classes of PCBs which correlations against p_L° are not able to explain, and partitioning of PCNs to Chicago aerosols is also accounted for by K_{OA} .

The K_{OA} absorption model described here requires knowledge of only K_{OA} and the organic matter fraction of the aerosol which are both more easily measurable than the parameters of the Junge–Pankow model. Thus, there is an incentive to utilize the absorption model for chlorinated aromatics and to measure K_{OA} as a function of temperature for other compounds of interest or concern.

Acknowledgments

We thank Tom Holsen (Illinois Institute of Technology, Chicago, IL) for arranging the sampling location in Chicago, Sherman R. Bauer (Illinois State Water Survey, Champaign, IL) for meteorological data, and Eva Jakobsson and Åke Bergman (Stockholm University) for their gifts of PCN congeners. This study was supported in part by the U.S. Environmental Protection Agency under contract CR-818834-01-0. This work has not been subjected to Agency review and therefore does not necessarily reflect the views of the Agency, and no official endorsement should be inferred.

Literature Cited

- Golomb, D.; Ryan, D.; Underhill, J.; Wade, T.; Zemba, S. *Atmos. Environ.* **1997**, *31*, 1361–1368.
- Holsen, T. M.; Noll, K. E.; Liu, S.-P.; Lee, W.-J. *Environ. Sci. Technol.* **1991**, *25*, 1075–1081.
- Offenberg, J. H.; Baker, J. E. *Environ. Sci. Technol.* **1997**, *31*, 1534–1538.

- (4) Gustafson, K. E.; Dickhut, R. M. *Environ. Sci. Technol.* **1997**, *31*, 140–147.
- (5) Halsall, C. J.; Barrie, L. A.; Fellin, P.; Muir, D. C. G.; Billeck, B. N.; Lockhart, L.; Rovinski, F.; Konovov, E.; Postoukov, B. *Environ. Sci. Technol.* **1997**, *31*, 3593–3599.
- (6) Stern, G. A.; Halsall, C. J.; Barrie, L. A.; Fellin, P.; Muir, D. C. G.; Billeck, B. N.; Lockhart, L.; Rovinski, E.; Konovov, E.; Postoukov, B. *Environ. Sci. Technol.* **1997**, *31*, 3619–3628.
- (7) Pankow, J. F. *Atmos. Environ.* **1987**, *21*, 2275–2283.
- (8) Pankow, J. F.; Bidleman, T. F. *Atmos. Environ.* **1992**, *25A*, 2241–2249.
- (9) Cotham, W. E.; Bidleman, T. F. *Environ. Sci. Technol.* **1995**, *29*, 2782–2789.
- (10) Falconer, R. L.; Bidleman, T. F.; Cotham, W. E. *Environ. Sci. Technol.* **1995**, *29*, 1666–1673.
- (11) Pankow, J. F. *Atmos. Environ.* **1994a**, *21*, 185–188.
- (12) Pankow, J. F. *Atmos. Environ.* **1994b**, *21*, 189–193.
- (13) Liang, C.; Pankow, J. F. *Environ. Sci. Technol.* **1996**, *30*, 2800–2805.
- (14) Odum, J. R.; Yu, J.; Kamens, R. M. *Environ. Sci. Technol.* **1994**, *28*, 2278–2285.
- (15) Paterson, S.; Mackay, D.; Bacci, E.; Calamari, D. *Environ. Sci. Technol.* **1991**, *25*, 866–871.
- (16) Tolls, J.; McLachlan, M. S. *Environ. Sci. Technol.* **1994**, *28*, 159–161.
- (17) Simonich, S. L.; Hites, R. A. *Environ. Sci. Technol.* **1996**, *28*, 2905–2914.
- (18) Finizio, A.; Mackay, D.; Bidleman, T. F.; Harner, T. *Atmos. Environ.* **1997**, *31*, 2289–2296.
- (19) Billings, W. N.; Bidleman, T. F. *Environ. Sci. Technol.* **1980**, *14*, 679–683.
- (20) Harner, T.; Bidleman, T. F. *Atmos. Environ.* **1997**, *31*, 4009–4016.
- (21) Shantz, M. M.; Parris, R. M.; Wise, S. A. *Chemosphere* **1993**, *10*, 1915, 1922.
- (22) Wise, S. A.; Hilpert, L. R.; Vogt, C. R.; Rebbert, R. E.; Lane, C. S.; Shantz, M. M.; Chesler, S. N.; May, W. E. *Anal. Chem.* **1988**, *332*, 573–582.
- (23) Simcik, M.; Zhang, H.; Eisenreich, S. J.; Franz, T. P. *Environ. Sci. Technol.* **1997**, *31*, 2141–2147.
- (24) Harner, T.; Bidleman, T. F. *J. Chem. Eng. Data* **1998**, *43*, 40–46.
- (25) Hanberg, A.; Wern, F.; Asplund, L.; Haglund, P.; Safe, S. *Chemosphere* **1990**, *20*, 1161–1164.
- (26) Pankow, J. F. *Atmos. Environ.* **1991**, *25A*, 2229–2239.
- (27) Hart, K. M.; Pankow, J. M. *Environ. Sci. Technol.* **1994**, *28*, 655–661.
- (28) Ligocki, M. P.; Pankow, J. F. *Environ. Sci. Technol.* **1989**, *23*, 75–83.
- (29) Falconer, R. L.; Bidleman, T. F. *Atmos. Environ.* **1994**, *28*, 547–554.
- (30) Yamasaki, H.; Kuwata, K.; Kuge, Y. *Nippon Kagaku Kaishi* **1984**, *8*, 1324–1329 (in Japanese).
- (31) Hinckley, D. A.; Bidleman, T. F.; Foreman, W. T. *J. Chem. Eng. Data* **1990**, *35*, 232–237.
- (32) Pankow, J. F. *Atmos. Environ.* **1988**, *22*, 1405–1409.
- (33) Holsen, T. M.; Noll, K. E.; Fang, G.-C.; Lee, W.-J.; Lin, J.-M.; Keeler, G. J. *Environ. Sci. Technol.* **1993**, *27*, 1327–1333.
- (34) Kamens, R. M.; Odum, J.; Fan, Z.-H. *Environ. Sci. Technol.* **1995**, *29*, 43–50.
- (35) Forstner, H. L.; Flagan, R.; Seinfeld, J. *Atmos. Environ.* **1997**, *31*, 1953–1964.
- (36) Bidleman, R. L.; Bidleman, T. F. In *Atmospheric Deposition of Contaminants to the Great Lakes and Coastal Waters*; Baker, J. E., Ed.; SETAC Press: Pensacola, FL, 1997; pp 151–170.
- (37) Harner, T.; Bidleman, T. F. *J. Chem. Eng. Data* **1996**, *41*, 895–899.
- (38) Junge, C. E. In *Fate of Pollutants in the Air and Water Environments*; Suffet, I. H., Ed.; Wiley-Interscience: New York, 1977; pp 7–26.
- (39) Bidleman, T. F. *Environ. Sci. Technol.* **1988**, *22*, 361–367.
- (40) Harner, T.; Mackay, D. *Environ. Sci. Technol.* **1995**, *29*, 1599–1606.
- (41) Kömp, P.; McLachlan, M. S. *Environ. Toxicol. Chem.* in press.
- (42) Bidleman, T. F.; Falconer, R. L.; Harner, T. In *Gas and Particle Partition Measurements of Atmospheric Compounds*; Lane, D. A., Ed.; Gordon and Breach Publishers: Newark, NJ (in press).
- (43) Bidleman, T. F.; Harner, T. In *Estimating Chemical Properties for the Environmental and Health Sciences: A Handbook of Methods*; Mackay, D., Boethling, R. S., Eds.; Ann Arbor Press: Chelsea, MI, 1997c; in press.
- (44) Gundel, L. A.; Lee, V. C.; Mahanama, K. R. R.; Stevens, R. K.; Daisey, J. M. *Atmos. Environ.* **1995**, *29*, 1719–1733.
- (45) Lane, D. A.; Gundel, L. *Polycyclic Aromat. Compd.* **1996**, *9*, 67–73.
- (46) Willeke, K.; Whitby, K. T. *J. Air Pollut. Control Assoc.* **1975**, *25*, 529–534.
- (47) Pankow, J. F.; Bidleman, T. F. *Atmos. Environ.* **1991**, *26A*, 1071–1080.
- (48) Shah, J. J.; Johnson, R. L.; Heyerdahl, E. K.; Huntzicker, J. J. *J. Air Pollut. Control Assoc.* **1986**, *36*, 254–257.
- (49) Jang, M.; Kamens, R. M.; Leach, K. B.; Strommen, M. R. *Environ. Sci. Technol.* **1997**, *31*, 2805–2811.

Received for review October 10, 1997. Revised manuscript received February 19, 1998. Accepted March 3, 1998.

ES970890R